Journal of Non-Crystalline Solids 401 (2014) 219–223

Contents lists available at ScienceDirect

Journal of Non-Crystalline Solids

journal homepage: www.elsevier.com/ locate/ jnoncrysol

Cross-sectional Raman micro-spectroscopy study of silver nanoparticles in soda–lime glasses

A. Quaranta [a,*], E. Cattaruzza [b], F. Gonella [b], A. Rahman [c,d], G. Mariotto [c]

[a] Department of Industrial Engineering, Università di Trento, Via Mesiano 77, I-38123 Trento, Italy
[b] Department of Molecular Sciences and Nanosystems, Università Ca' Foscari Venezia, I-30123 Venezia, Italy
[c] Department of Informatics, University of Verona, Strada Le Grazie 15, I-37134 Verona, Italy
[d] Department of Applied Physics and Electronic Engineering, University of Rajshahi, Rajshahi 6205, Bangladesh

ARTICLE INFO

Article history:
Received 27 September 2013
Received in revised form 8 December 2013
Available online 19 January 2014

Keywords:
Ion exchange;
Silicate glasses;
Nanoclusters;
Micro-Raman

ABSTRACT

The growth and distribution of silver nanoparticles in ion exchanged glasses induced by thermal treatments in air at different temperatures were studied by means of cross-sectional Raman micro-spectroscopy analysis. Silver–sodium ion exchange of commercial soda–lime silicate glasses was done at 320 °C for 20 min, then the samples were treated by thermal annealing in air at temperatures in the range between 400 and 550 °C for 1 h. During the post-exchange thermal treatment, a further diffusion of silver from the surface toward the bulk occurred, together with the progressive formation of silver nanoparticles, whose fractional amount increased with an increase of the annealing temperature. Their average size and the related evolution as a function of the depth and of the treatment temperature were determined by Raman micro-spectroscopy analysis of the sample cross-section. Both aggregation of silver species and growth of silver nanoclusters are discussed on the basis of the theory of homogeneous nucleation in solids.

1. Introduction

In spite of the considerable amount of experimental research performed in the last two decades, the controlled doping of silicate glass waveguides with metal nanoclusters is still a challenging task for applications in several fields, such as photonics, catalysis and sensor technology, and for the preparation of superparamagnetic materials [1–4]. Furthermore, metal nanoclusters can induce a significant enhancement of the luminescence properties of rare earths in glasses, due to the widening of the excitation bandwidth [5,6], which is of crucial importance in telecommunication technology. In order to get the control of the size and distribution of nano-aggregates in the glass matrix, the precipitation of metal or oxide nanoparticles in glasses has been studied from more basic viewpoints, with specific concern for the cluster nucleation and growth kinetics, stability, and structure in terms of composition, crystalline phase, size, and size distribution [7–11].

In particular, for most applications it is of outmost importance to obtain optical waveguides containing nanoclusters with concentration and size sufficiently small to prevent significant attenuation of the transmitted light signal intensity. In this respect, the ion exchange process (either thermally or field-assisted driven) has demonstrated to be a peculiarly effective technique for doping silicate glasses well beyond the dopant solubility limits, thus producing glass light waveguides in which the formation of nanoparticles may be subsequently promoted by suitable energetic treatments, like irradiation with light ions [12,13], heat treatments in a reducing atmosphere [14,15] or by means of laser irradiation [16,17].

Silver has been the most studied element as metal dopant for these systems, since it is used for the production of several passive and active waveguiding glass-based devices, and its aggregation in the waveguides can be induced by means of several — possibly combined — procedures.

In spite of this great deal of studies, a complete phenomenological description of the nucleation and growth of metal clusters upon ion exchange and thermal annealing for silver-containing waveguides is still lacking, due to several factors. Indeed, ion exchange is intrinsically a non-equilibrium process, where at least three phenomena contribute to give the final system, namely, diffusion, nucleation and aggregates growth. These processes exhibit different regimes, that can be somewhat competing. This happens when dynamic feedbacks are triggered, either weakening or enhancing one process upon small changes of the involved variables like for example the local silver concentration, the temperature, the glass composition, or even the local stoichiometry.

The literature on the aggregation of silver in glass highlights in turn different aspects. The combination of diffusion, aggregation and growth phenomena was first faced by Berger [7], neglecting the diffusion of Ag^0 in the glass matrix, while several other works [8–11] studied the behavior of silver in ion exchanged systems taking into account both the diffusion and the reduction mechanisms, considering also the diffusion coefficient of reduced silver. In this case, the problem is quite complex due to the additional contribution of hydrogen. Nonetheless, the growth

* Corresponding author at: Università di Trento, Dipartimento di Ingegneria Industriale, Via Mesiano 77, 38123 Povo, Trento, Italy. Tel.: +39 0461 282450; fax: +39 0461 281945.
E-mail address: quaranta@ing.unitn.it (A. Quaranta).

0022-3093/$ – see front matter © 2014 Elsevier B.V. All rights reserved.
http://dx.doi.org/10.1016/j.jnoncrysol.2013.12.041

of nanoparticles within an ion-exchanged glass induced only by thermal treatments is still a rather unexplored task [18,19]. It is worth noting that the reduction of silver in silicate glasses can occur even without reducing agents, owing to the presence in the silica network of loosely bound electrons in reducing defects [20]. In fact, the formation of silver nanoparticles in as-exchanged glasses has been recently experimentally revealed by micro-Raman analysis of ion exchanged waveguides [19].

In this framework, the use of spectroscopic techniques in a configuration that allows a cross-sectional analysis is expected to give novel contributions in the understanding of the mechanisms underlying the formation of metal nanoparticles. In this paper, micro-Raman spectroscopy analyses are presented for silver–sodium ion-exchanged silicate glass slides. To this aim, both front-face and cross-section measurements were performed on the samples after the ion exchange process, as well as after thermal treatments in air at different temperatures. The particle size was calculated from the position of the maximum of low-frequency Raman peak. Then, the growth mechanism of the nanoparticles was described for different silver concentrations and as a function of both the temperature and the involved activation energies, estimated in the frame of the homogenous nucleation model.

2. Experimental

Commercial optical soda–lime glass (SLG) slides, of atomic composition O 60%, Si 24%, Na 10%, Mg 2.3%, K 2.0%, Ca 1.0%, Al 0.7% plus impurity traces, were immersed for 20 min in a molten salt bath of $AgNO_3$: $NaNO_3$ (1.0 mol%) at 320 °C. Some samples were then annealed in air for 1 h, at fixed temperatures in the range between 400 and 550 °C with steps of 50 °C.

Cross-polarized micro-Raman spectra were taken at room temperature in backscattering geometry using a triple-axis monochromator (Horiba-Jobin Yvon, model T64000), set in double-subtractive/single configuration, and equipped with three holographic gratings of 1800 lines/mm. The spectra were excited by the 514.5 nm line of a mixed Ar–Kr ion gas laser. The laser beam was focused onto the sample surface over a region of about 1 μm in size, and the scattered radiation from this region was collected in confocal mode exploiting the same objective used to focus the incident laser beam.

The sample characterization was performed in confocal mode by analyzing both the exchanged glass surface and the sample cross-section for in-depth investigation of the exchanged layer.

For the first type of measurements, the laser beam was focused onto the sample surface through the lens of a 100× microscope objective (N.A. = 0.90). In this configuration, the size of the spot was set in order to focus the laser light on the outermost part of the glass slide.

As for in-depth resolved micro-Raman profiling of glass layers, a cross-sectional cut of as-exchanged and thermally treated samples was first performed, and then confocal Raman microspectroscopy (CRM) was adopted for the lateral scanning throughout the cross-section of the glass layers. An 80× microscope objective (N.A. = 0.75) was used to excite and collect the Raman spectra for in-depth profiling measurements.

Sample positioning under the microscope objective was achieved by a manually operated X–Y translator, with sub-micrometric resolution. In-depth profiling analyses were performed by recording the low frequency Raman scattering spectra along the section perpendicular to the surface of the glass slide, starting from its edge by steps of few microns toward the inner region. The laser power on the sample surface was kept below 1 mW, to avoid heating effects. The scattered radiation, filtered by a double-monochromator, was detected by a liquid nitrogen cooled CCD detector and the final resolution was better than 0.6 cm^{-1}/pixel. In order to accurately determine the low frequency peak wavenumber, different emission lines from the neon lamp were used as reference. Repeated micro-Raman measurements on different sample regions, lying at the same depth beneath the sample surface, were run under the same experimental conditions, verifying that the recorded spectra exhibit a very good reproducibility.

3. Results

After the ion exchange process, the glass samples were colorless, without exhibiting absorption features in the visible region. After the thermal annealing at temperatures higher than 400 °C, the glasses turned yellowish, with color density increasing with the temperature.

Low-frequency cross-polarized micro-Raman spectra acquired for the surface of bare, as-exchanged and thermally treated glasses are reported in Fig. 1.

As it can be observed, the bare glass exhibits the so-called boson peak, which is characteristic of the disordered systems, in the form of a broad bump with maximum at about 60 cm^{-1}. After Ag^+ ion exchange, a distinct low-frequency Raman band peaking at about 32 cm^{-1} clearly grows up. The samples annealed up to 400 °C (not shown in the figure) exhibit the same features of the as-exchanged sample, along with a progressively enhanced luminescence background extending to the high wavenumber side. At annealing temperatures higher than 400 °C, the low-frequency Raman band increases in intensity, sharpens and progressively shifts toward lower wavenumbers.

The observed low-frequency Raman scattering is due to the acoustic vibrational modes of metal silver nanoparticles embedded in the soda–lime silicate glass matrix. In particular, within the approximation of spherical particle shape, the peak frequency ω_p can be related to the particle diameter d by the relationship [21]:

$$d = 0.85\frac{v_t}{\omega_p c} \tag{1}$$

where v_t is the transverse sound velocity in silver (1660 m/s) and c is the light speed. A shift to lower wavenumbers of this peak can be therefore ascribed to an increase of the mean particle size, while its intensity is proportional to particle volume.

Hence, the low-frequency Raman spectra suggest that just beneath the surface of the as-exchanged glass a low concentration of small silver nanoparticles is present, whose average size increases with the annealing temperature. The width of the peaks and the tail toward higher wavenumbers indicates the presence of small particles with a broad size distribution in the sample annealed at 450 °C. The size distribution becomes narrower on further increasing the annealing temperature. The average dimension of the particles on the surface of the glass, as calculated from Eq. (1), ranges from 1.5 nm for the as-exchanged

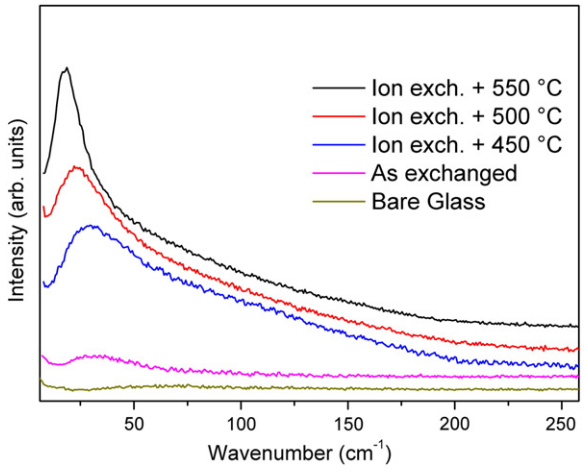

Fig. 1. Low-frequency cross-polarized micro-Raman spectra of the bare soda–lime silicate glass, as-exchanged glass, and ion exchanged glass after annealing in air for 1 h at different temperatures. for 1 h.

sample to 2.6 nm for the sample annealed at 550 °C, with the values of 1.6 nm and 2.2 nm for the samples annealed at 450 °C and 500 °C, respectively.

In Fig. 2a–c part of the low-frequency Raman spectra at different depths, collected from the as-exchanged sample and from the exchanged samples treated at 450 °C and 550 °C, are shown. In the as-exchanged sample (Fig. 2a) the low-frequency Raman peak broadens, decreases in intensity and also slightly shifts toward higher frequencies on increasing the depth within the bulk. The observed spectral changes as a function of depth indicate that the size of the particles decreases by increasing the depth, passing from the average value of 1.5 nm at the sample surface to the value of 1.0 nm starting at about 5 μm depth.

After annealing at 450 °C, the peak is still rather broad and is accompanied by more or less pronounced shoulders on the higher wavenumber side (Fig. 2b), reflecting an increase of the fractional amount of small clusters in the glass matrix. Moreover, the peak position does not change up to the maximum depth at which the presence of Ag nanoparticles can be detected, which turns out to be higher with respect to the as-exchanged sample (13 μm vs. 6 μm). Finally, a different behavior is observed by increasing the temperature of the sample treatment, as it can be seen in Fig. 2c. In fact, for the sample heated at 550 °C for 1 h, the peak progressively sharpens and shifts toward lower wavenumbers by increasing the probed depth, up to about 24 μm, thus indicating that the particle dimension increases with a sharper size distribution throughout the silver distribution profile. The average particle diameter, derived from the position of the low-frequency peak according to Eq. (1), increases from 2.6 nm at the sample surface up to 3.8 nm at a depth of about 24 μm. In particular, this average particle size remains constant at depths higher than 20 μm.

4. Discussion

Nucleation and growth of nanoparticles in a glass matrix is usually treated with the homogenous nucleation model, where nuclei appear into a homogenous solution without any seed for heterogeneous nucleation, like dust, particles or bubbles [22]. In this framework, the formation and growth of nanoparticles occur by means of a diffusion-controlled process underlying three distinct precipitation steps, namely nucleation, normal growth and competitive growth. At a first step, small nuclei are formed. Thereafter, at a second step, crystallites grow in a supersaturated system by capturing the diffusing atoms from the matrix. Finally, when the particles are large enough and the supersaturation degree is negligible, the growth is governed by the diffusive mass transfer from smaller particles to larger ones (Ostwald ripening).

In silver ion-exchanged glasses, Ag^0 atoms are formed by reaction of Ag^+ ions with electron donor defects in the silica network and promptly aggregate into small nuclei since the solubility of metallic silver in glass is very small. In other words, the supersaturation of metallic silver in glass is very high, so stable clusters are formed with a very small radius, typically of few tenths of nm.

After this stage, the cluster diameter d grows with the time by diffusion of Ag^0 to the surface of the stable nuclei, following the relationship [9,22–24]:

$$d^2 = d_0^2 + 8Dt\frac{C_0 - C_e}{C_\beta - C_e} \quad (2)$$

where d_0 is the value of the particle diameter at $t = 0$, C_0, C_e and C_β are the Ag^0 concentrations in the matrix at $t = 0$, at the equilibrium and within the particle, respectively, and D is the diffusion coefficient of atomic silver. This last parameter varies exponentially vs. the temperature: i.e., $D = D_0\exp(-\Delta G_m / kT)$, where D_0 is the pre-exponential factor and ΔG_m is the energy barrier for the jump of Ag^0 from site to site through the network.

In ion-exchanged glasses during the heat treatments, the diffusion of Ag^+ allows the formation of atomic silver in the matrix by the reducing

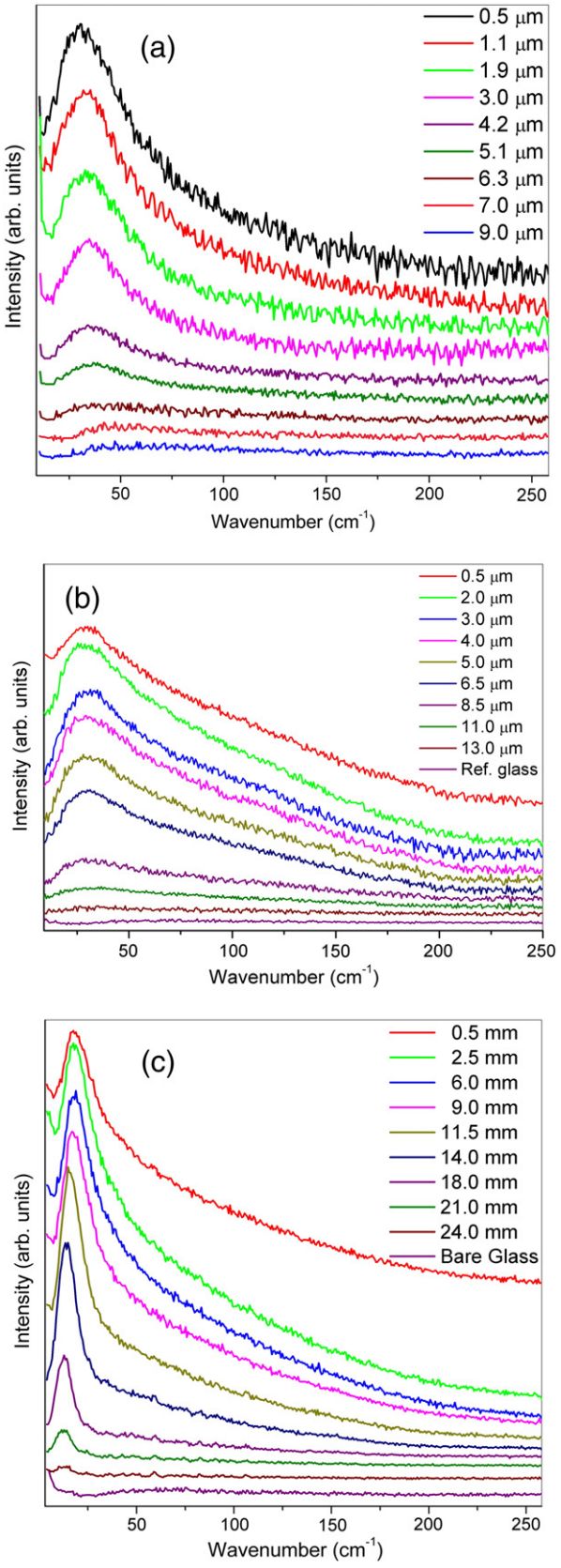

Fig. 2. Low-frequency cross-polarized Raman spectra recorded at different probed depths on: as-exchanged glass (a), sample after thermal annealing at 450 °C (b), and sample after thermal annealing at 550 °C (c). Spectra in each panel were vertically translated for the sake of clarity.

centers, so it can be assumed at a first approximation that the supersaturation does not decrease during the process, treating the cluster growth by Eq. (2) and neglecting the Ostwald ripening mechanism. Moreover, C_0 can be considered constant within depth intervals that are smaller than the silver diffusion length, but larger than the particle size, as it is a necessary condition for Eq. (2) to subsist.

Under these conditions, we can analyze the activation energy of the process by drawing an Arrhenius plot of $\ln(d^2-d_0^2)$ vs. $(kT)^{-1}$ for different depths, where d_0 is the particle size in the as-exchanged glass, when particles are present, being 0 at depths higher than the maximum depth in the as-exchanged sample. In Fig. 3, the Arrhenius plots are reported, calculated for the particle diameters at the surface and at the depth of about 12 μm, respectively.

In Fig. 4, the calculated values are shown for the activation energy at different depths, where the error bars were obtained by the fitting program. As it can be observed, the activation energy decreases from the surface to the depth of 12 μm, ranging from 1.2 ± 0.3 eV to 0.6 ± 0.2 eV. The values near the surface are in good agreement with the activation energy of about 1.0 eV calculated for the diffusion of ionic silver [14,25,26]. At higher depths, where the starting concentration of Ag^+ before the heat treatment was negligible, the activation energy is lower, as reported in the literature for Ag^0 extrapolated values [9,27].

The formation and aggregation of metallic silver are a quite complex process: during the heat treatment, ionic silver diffuses into the glass slides, substituting Na^+ in the alkali sites, owing to the concentration gradient in the concentration profile. At the same time, Ag^+ is reduced into Ag^0 by the network defects, starting to aggregate into nanoparticles. In the regions where the starting ionic concentration is quite high, Ag^+ can be reduced during its path close to a particle, being thereafter captured as Ag^0. This is the reason why in these regions the activation energy is so similar to that of ionic silver: the actual diffusion coefficient related to the particles growing up is that of Ag^+. At higher depths, the silver is supplied as for the starting concentration profile, and it is mostly reduced far before reaching the particle region, so the diffusion coefficient governing the process is mainly that of Ag^0, and the activation energy lowers.

As far as the particle size is concerned, it is related to the concentration of nucleating centers as a function of the depth in as-exchanged samples. It is quite established that nucleation centers in silver exchanged glasses are dimers or trimers, like $(Ag_3)^{2+}$, which are formed in the glass network near reducing defects [28]. It is reasonable to assume that the amount of nucleation centers is higher where the silver concentration is higher; for this reason in the near surface region the particle growth is hindered by the competition between the clusters,

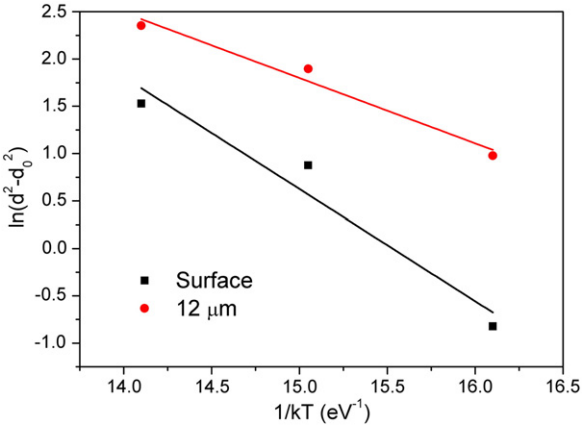

Fig. 3. Arrhenius plot of the particle diameters at the surface (black squares) and at the depth of 12 μm (red circles). Solid lines are the linear fit curves.

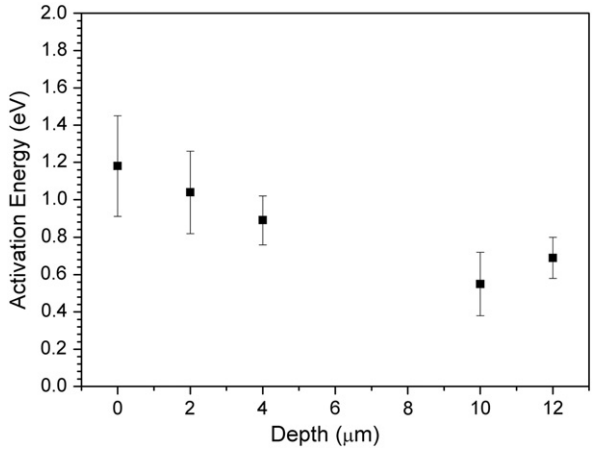

Fig. 4. Activation energy values as a function of the depth calculated from the Arrhenius plots.

giving rise to a smaller average size. On the other hand, at higher depth the lower amount of nucleation centers allows the particle growth resulting in a larger dimension of the cluster size. Any role of atmospheric oxygen can be ruled out in this work, since the oxygen diffusivity in glass is too low to affect the oxidation state of silver at the penetration depths reached in the examined samples.

It is worth stressing that the used configuration for cross-sectional Raman micro-spectroscopy provides information on the glass structure as a function of the depth averaged over a relatively large region, so preventing local fluctuations of collected data. Moreover, it does not require sophisticated sample preparation nor long time analysis and, besides the information concerning the size and size distribution of nanoparticles, on which this work is mainly focused, can be also exploited [19] for determining the role played by the glass defects population, as well as by the ion exchange regime in terms of local silver concentration and local modification and degree of polymerization of the silicate network.

5. Conclusions

In this work, the formation of silver nanoparticles by thermal annealing in air of ion exchanged glass waveguides has been analyzed with cross-sectional micro-Raman spectroscopy on the distribution profiles. In the as-exchanged sample, small nanoparticles are present with size decreasing with the depth, while during the heat treatments silver diffuses into the glass and the particle size increases from the sample surface to different depth values. The process has been analyzed in the framework of the homogenous nucleation model, and the activation energy for the particle growth has been calculated at different depths. Near the surface, where the ionic silver concentration is high, the activation energy is similar to that of Ag^+ diffusion coefficient, thus indicating that the diffusion of the ionic species leads the growth mechanism. On the other hand, at higher depths the activation energy is more similar to the literature values for Ag^0 diffusion, suggesting that the process is governed mainly by the diffusion of the neutral species formed by reduction of Ag^+ with defects of the glass network. The cluster size is mainly related to the amount of nucleation centers: owing to competing growth mechanisms, the higher the concentration of centers the lower the particle size turns out to be.

Since the silver diffusion and reduction process studied in this work involves depths of few tens of microns, it is reasonable to assume that the conclusions and the enlightened mechanisms are relevant for any kind of shape of glass samples, like fibers or cylinders. A further study should be performed for channel waveguides, where the channel dimensions are comparable or even lower with respect to the involved depths and important lateral diffusion effects are present.

A deeper understanding of the process will be further developed by using diffusion reaction equations, being the Ag^0 diffusion activation energy usually extrapolated after simplifying assumptions, so a more complete study of the process accounting for the diffusion and reduction mechanisms is in progress. Finally, cross-sectional Raman microspectroscopy has been demonstrated to be an effective analytical technique for the analysis of doped glasses.

References

[1] P. Mazzoldi, G.W. Arnold, G. Battaglin, F. Gonella, R.F. Haglund Jr., J. Nonlinear Opt. Phys. Mater. 5 (1996) 285.
[2] C. de Julián Fernández, C. Sangregorio, G. Mattei, G. De, A. Saber, S. Lo Russo, G. Battaglin, M. Catalano, E. Cattaruzza, F. Gonella, D. Gatteschi, P. Mazzoldi, Mater. Sci. Eng. C 15 (2001) 59.
[3] C. de Julián Fernández, G. Mattei, C. Maurizio, E. Cattaruzza, S. Padovani, G. Battaglin, F. Gonella, F. D'Acapito, P. Mazzoldi, J. Magn. Magn. Mater. 290–291 (2005) 187.
[4] Y. Yamamoto, H. Hori, Rev. Adv. Mater. Sci. 12 (2006) 23.
[5] A. Martucci, M. De Nuntis, A. Ribaudo, M. Guglielmi, S. Padovani, F. Enrichi, G. Mattei, P. Mazzoldi, C. Sada, E. Trave, G. Battaglin, F. Gonella, E. Borsella, M. Falconieri, M. Patrini, J. Fick, Appl. Phys. A 80 (2005) 557.
[6] F. Gonella, Rev. Adv. Mater. Sci. 15 (2007) 134.
[7] A. Berger, J. Non-Cryst. Solids 151 (1992) 88.
[8] A. Miotello, G. De Marchi, G. Mattei, P. Mazzoldi, Appl. Phys. A 67 (1998) 527.
[9] A. Miotello, G. De Marchi, G. Mattei, P. Mazzoldi, A. Quaranta, Appl. Phys. A 70 (2000) 415.
[10] Yu. Kaganovskii, A. Lipovskii, M. Rosenbluh, V. Zhurikhina, J. Non-Cryst. Solids 353 (2007) 2263.
[11] A.V. Redkov, V.V. Zhurikhina, A.A. Lipovskii, J. Non-Cryst. Solids 376 (2013) 152.
[12] G.W. Arnold, G. De Marchi, F. Gonella, P. Mazzoldi, A. Quaranta, G. Battaglin, M. Catalano, F. Garrido, R.F. Haglund Jr., Nucl. Instr. Meth. B 116 (1996) 507.
[13] A.E. Volkov, D.N. Korolev, Nucl. Instr. Meth. B 209 (2003) 98.
[14] G. De Marchi, F. Caccavale, F. Gonella, G. Mattei, P. Mazzoldi, G. Battaglin, A. Quaranta, Appl. Phys. A 63 (1996) 403.
[15] C. Mohr, M. Dubiel, H. Hofmeister, J. Phys. Condens. Matter 13 (2001) 525.
[16] F. Gonella, P. Mazzoldi, in: H.S. ìNalwa (Ed.), Handbook of Nanostructured Materials and Nanotechnology, vol. 4, Academic Press, San Diego, 2000.
[17] E. Trave, F. Gonella, P. Calvelli, E. Cattaruzza, P. Canton, D. Cristofori, A. Quaranta, G. Pellegrini, Nucl. Instr. Meth. B 268 (2010) 3177.
[18] E. Borsella, E. Cattaruzza, G. De Marchi, F. Gonella, G. Mattei, P. Mazzoldi, A. Quaranta, G. Battaglin, R. Polloni, J. Non-Cryst. Solids 245 (1999) 122.
[19] A. Quaranta, A. Rahman, G. Mariotto, C. Maurizio, E. Trave, F. Gonella, E. Cattaruzza, E. Ghibaudo, J.E. Broquin, J. Phys. Chem. C 116 (2012) 3757.
[20] R.J. Araujo, Appl. Opt. 31 (1992) 5221.
[21] M. Ferrari, F. Gonella, M. Montagna, C. Tosello, J. Appl. Phys. 79 (1996) 2055.
[22] S.V. Gaponenko, Optical Properties of Semiconductor Nanocrystals, Cambridge University Press, Cambridge, UK, 1998. (ch. 3).
[23] H.B. Aaron, D. Fainstein, G.R. Kotler, J. Appl. Phys. 41 (1970) 4404.
[24] H. Yukselici, P.D. Persans, T.M. Hayes, Phys. Rev. B 52 (1995) 11763.
[25] J.L. Barton, M. Morain, J. Non-Cryst. Solids 3 (1970) 115.
[26] G. Battaglin, G. Della Mea, G. De Marchi, M. Guglielmi, P. Mazzoldi, A. Di Martino, J. Non-Cryst. Solids 95–96 (1987) 1079.
[27] P. Gangopadhyay, P. Magudapathy, R. Kesavamoorthy, B.K. Panigrahi, K.G.M. Nair, P.V. Satyam, Chem. Phys. Lett. 388 (2004) 416.
[28] A.V. Dmitryuk, S.E. Paramzina, A.S. Perminov, N.D. Solov'eva, N.T. Timofeev, J. Non-Cryst. Solids 202 (1996) 173.